Korean J. Chem. Eng., **29**(2), 139-144 (2012)
DOI: 10.1007/s11814-011-0159-5

Experimental investigation of explosion pressures and flame propagations by wall obstruction ratios and ignition positions

Dal Jae Park and Young Soon Lee†

Department of Safety Engineering, Seoul National University of Science and Technology, Seoul 139-743, Korea
(*Received 15 December 2010 • accepted 13 June 2011*)

Abstract−Experimental studies were carried out to investigate the effects of different ignition source locations and wall obstructions in a partially opened chamber, 235 mm in height, with a 1,000×950 mm^2 cross section and with a large top-venting of area of 1,000×320 mm^2. Four different ignition positions such as the bottom, side, corner and top, and three wall obstacles with blockage ratios ranging from about 10 to 30% were used. The comparisons between wall obstacles in the chamber showed that the dependence of overpressure on obstruction ratios was different compared with published experiments with a large L/D ratio enclosure. This may be linked to the characteristics of the chamber. The smallest wall obstacle caused the highest overpressure, while the largest one caused the lowest overpressure. The flame propagation and pressure development were highly sensitive to the ignition positions. The bottom ignition caused the highest overpressure, while the top ignition the closest to the vent opening caused the lowest overpressure.

Key words: Ignition Locations, Solid Obstacles, Flame Propagation, Overpressure

INTRODUCTION

The most severe threat to industries such as petrochemical, gas utilities, and coal mining is the hazard of gas explosions. The severity of such explosions is dependent on the fuel reactivity, obstacle density, confinement, and so on. In particular, explosions occurring in confined and partially opened regions are of special focus due to the potential for domino effects and more serious consequences. Therefore, prediction of overpressures occurring due to the explosions is important for the design of equipment, safety cases and emergency planning.

Park and Lee [1] mentioned that the most effective approach among different theoretical models for predicting the behavior of gas explosions is computational fluid dynamics. The accuracy of a CFD simulation is limited by the accuracy of the numerical model and the underlying physical sub-models such as combustion and turbulence [2]. The CFD models should be validated against sufficient experimental data before it can become a useful model. However, the CFD models currently available have been tested against limited experimental data. Thus, experimental studies are required to further understand the physical processes, and the data gained is crucial for the validation of physical sub-models of CFD.

Experimental investigations on the effect of ignition point positions and obstacles of factors influencing the explosion strength are continual outstanding research issues which need to be resolved in order to improve current CFD model capabilities. In the last thirty years, the majority of both large- and small-scale experiments have been performed to investigate the interaction between the propagating flame and obstacles inside various enclosures with large L/D (length to diameter ratio). Most investigators [3-7] reported that there is a strong interaction between the turbulence level formed behind the obstacle and the resulting peak pressure. For experiments on the effect of ignition point positions, early experiments [8,9] showed that the ignition positions influenced the explosion duration, the peak pressure and flame development. The studies of Solberg et al. [10] to investigate the effects of central and rear ignition within a 35 m^3 vessel revealed that the rear ignition caused lower pressures than those with central ignition close to the vent opening because hot combustion gases are vented at high velocities in the rear ignition. The experiments of Phylaktou and Andrews [3] performed in long closed vessels found that small changes in the spark position had a very significant effect on flame speed and initial rate of pressure rise. Also, the studies of Green and Nehzat [11] performed in a multi-channel model showed that higher pressures were shown due to the flow distortion ahead of flame when ignition occurred further away from the vent. Recently, Kindracki et al. [12] reported that the flame propagation and pressure variation in an elongated explosion vessel with/without obstacles are very sensitive to the positions of the ignition, and the size and the shape of the obstacles.

Most measurements of obstacles and ignition locations on explosion development mentioned above have been done in enclosures with large L/D. Their results revealed that the turbulent flame and turbulence interaction trapped behind the obstacle greatly enhance the speed of flame propagation and hence increase the rate of pressure rise, and the flame propagation and explosion pressures are highly dependent on the locations of the ignition point in large L/D chambers.

However, the influences of different ignition positions and different wall obstructions on both the flame propagation and explosion pressure in a partially opened enclosure with small L/D ratio and large top venting area have not been studied. The main objectives in this work are to investigate the underlying mechanisms of the phenomena observed on both the flame propagation and explosion pressure by wall obstructions and different ignition positions in premixed methane-air mixtures in a partially opened chamber

†To whom correspondence should be addressed.
E-mail: lysoon@snut.ac.kr

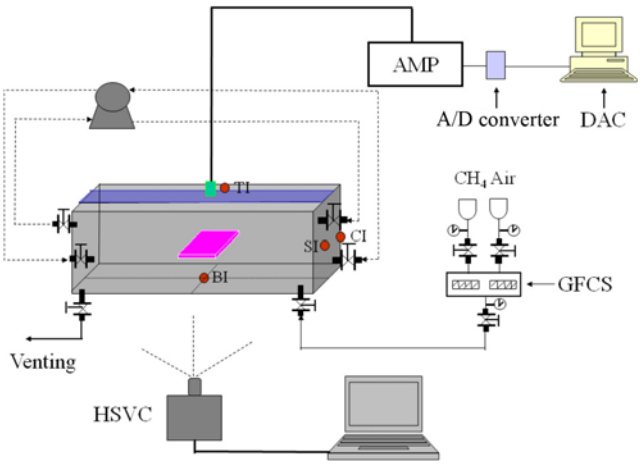

Fig. 1. Schematic diagram of the experimental set-up.

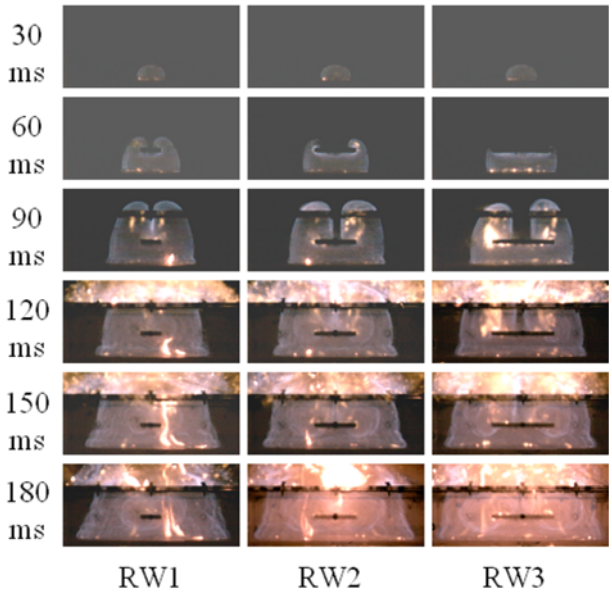

Fig. 2. A sequence of selected high-speed images of flame propagation with rectangular obstacles: RW1 (B.R.=10%), RW2 (B.R.=20%) and RW3 (B.R.=30%).

with small L/D ratio and large vent area, and to provide experimental data necessary for the further validation of physical sub-models of CFD.

EXPERIMENTAL

The fuel-air mixture, apparatus and experimental methods used in this work are the same with the measurements described in previous work [13]. Fig. 1 shows a schematic of the experimental set-up. As shown in Fig. 1, four different ignition positions representing bottom ignition (BI), corner ignition (CI), side ignition (SI) and top ignition (TI) were chosen. Table 1 indicates different solid wall obstruction ratios ranging from 10% to 30%. The obstacles used in this study are the same as those used in studies of Park et al [14].

RESULTS AND DISCUSSION

1. Influence of Wall Obstructions

Fig. 2 shows a sequence of selected high-speed images of flame propagation involving rectangular obstacles with blockage ratios ranging from 10 to 30%. Table 2 shows travel times of flame impingement on the obstacles, flame reconnection times in the wake of the obstacles and the delay times for the flame to vent for the obstacles used. The time shown represents the elapsed time after ignition and subsequent flame images at 30 ms intervals between 30 ms and 180 ms.

The flame in the early stages of flame movement develops hemispherically in a similar manner to the laminar flame from the ignition point. As indicated in Table 2, the propagating flame fronts reached the nearest face of the obstacle from the ignition point at around 38-40 ms for the different obstruction ratios. The flame arrival at the obstacle was almost similar, regardless of the obstruction ratios used. After impinging on the obstacle, the flame front emerged from the large gap between the obstacle and the chamber side walls causing a series of vortex pairs around the obstacle.

With increasing time, the flame starts to roll up in the wake of the obstacle. Flame reconnection in the wake of the obstacle for three configurations occurred between 62-84 ms after ignition. Note that the flame reconnection in the RW2 and RW3 occurred outside the chamber after the propagating flame front approached the chamber exit. The fastest flame reconnection occurred with the blockage

Table 2. Travel time for the flame to reach the nearest face of the rectangular obstacle, the flame reconnection time behind the obstacles, and the delay time before the flame exits the chamber after ignition

	RW1 [13]	RW2	RW3
a	38	38	40
b	62	80*	84*
c	70	74	78

*: Flame-front reconnection occurs outside the chamber vent
a: Travel time for the flame to reach the nearest face of the obstacle (ms)
b: Flame reconnection time (ms)
c: The delay time before the flame exits the chamber (ms)

Table 1. The different solid wall obstacles used in the explosion chamber

Obstacle type	Symbol	Dimensions (mm)	Blockage ratio (%)
Rectangular wall obstacles	RW1	Length 950×width 100×height 20	10
	RW2	Length 950×width 200×height 20	20
	RW3	Length 950×width 300×height 20	30

ratio of 10% (RW1), while the slowest flame reconnection occurred with the blockage ratio of 30% (RW3). The travel time of the propagating flame front to the chamber exit was around about 70-78 ms after ignition. Like flame reconnection time, the fastest time of the flame exiting the chamber occurred with the lower blockage ratio rather than the higher blockage ratio. The reason arises because the propagating flame was not fully developed due to the distance from ignition point to the chamber exit being too short. As the flame front reached the chamber exit, the propagating flame front was moved laterally along the vent with an increase in flame surface area, pushing unburnt mixture ahead of it. Air outside the chamber entered at the side of the vent away from the flame front. The interaction of flame around the obstacle with the vent caused complex vortices to form as flame spread along the obstacle towards the side of the chamber.

Fig. 3 shows the variations of flame height and width of the propagating flame front for rectangular plate obstructions of 10%, 20% and 30%. Here, the flame height was measured as the tip of the flame front above the base of the chamber until the flame front exited the chamber and the flame width was measured as the lateral width of the flame at the base of the chamber. The longest flame height and width within the chamber were obtained with the RW3 of the blockage ratio of 30%, being 275 and 514 mm, at about 64 ms after ignition. However, the shortest flame height and width occurred with the RW1 with the blockage ratio of 10%, being 208 and 391 mm, at about 64 ms. As the blockage ratio increased, the flame development of the flame height and width was proportional to the obstruction ratio.

Although the variations in the flame heights and flame widths of the different obstruction ratios were small compared to those obtained from explosion tests by Masri et al. [6], the results have a similar trend with their results. However, the volume of unburnt mixture in chamber which has very small L/D ratios of 0.235 and large rectangular top-venting may be different from that published in the literature for large L/D. For this measurement, as the propagating flame front reached the chamber exit, the flame front moved laterally along the vent. And the unburnt gas between the propagating flame and the side walls of the chamber was pushed by the lateral flame spread through the chamber exit. The RW3 with the faster increase in the flame height and width may have caused lower volumes of unburnt gas within the chamber while the RW1 with the slower increase caused higher volumes. Thus, the faster development in the flame height and width may have resulted in the expulsion of a larger volume of the unburnt gas within the chamber through the chamber exit as well as increasing the inflow of air into the chamber, as in the studies of Park et al. [13].

Fig. 4 shows the influence of the rectangular wall obstructions on explosion development. Here, the pressure data of the RW1 were taken from the experiments of Part et al. [13]. The pressure development was constant for given blockage ratios until about 100 ms in the experiments after which the pressure diverged. The RW1 with the blockage ratio of 10% caused the highest overpressure: 97 mbar at 224 ms. The RW3 with the blockage ratio of 30% caused the lowest overpressure: 67 mbar at 274 ms. As the obstruction ratio within the chamber increased, the explosion pressure decreased. The time taken to reach the maximum pressure was also found to be shorter with the lower obstruction ratio rather than the higher obstruction ratio. The pressure developments obtained from the different wall obstruction ratios within the chamber with low L/D used in this study

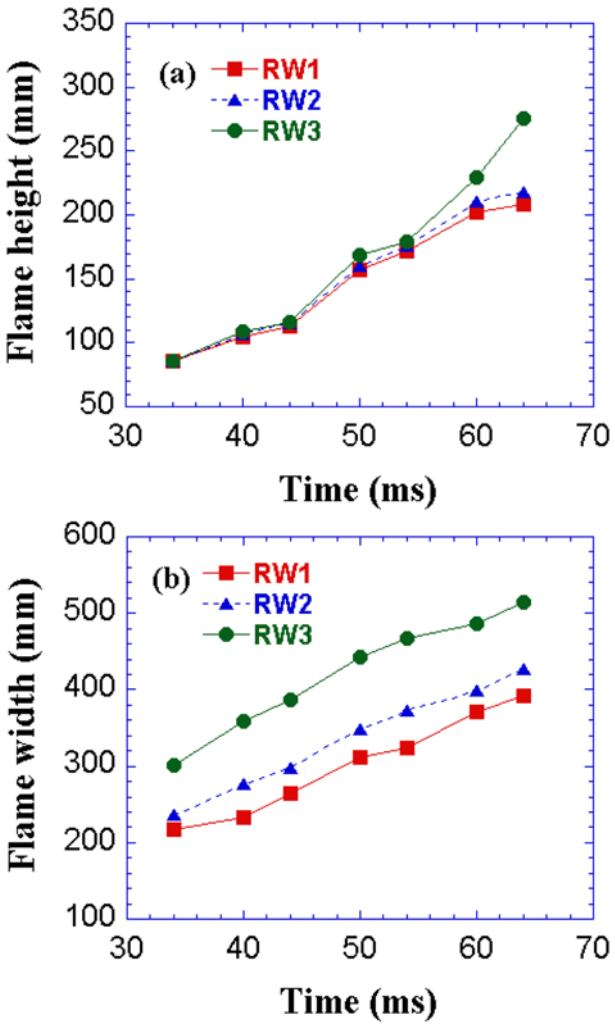

Fig. 3. Flame height and width with time for the rectangular obstacle obstructions: (a) flame height and (b) flame width.

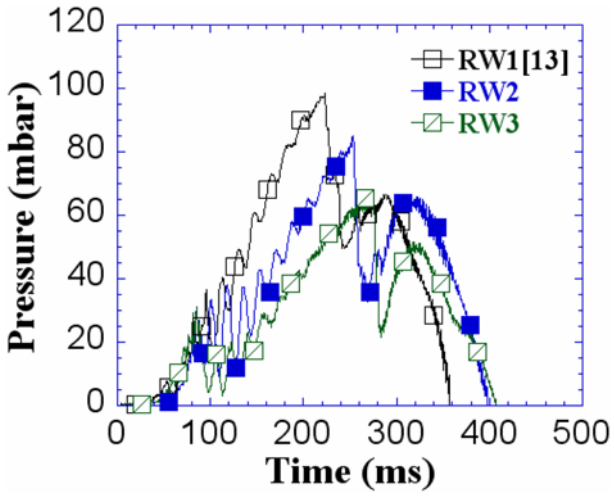

Fig. 4. Comparison of the pressure-time history for rectangular obstacles (RW1, RW2 and RW3).

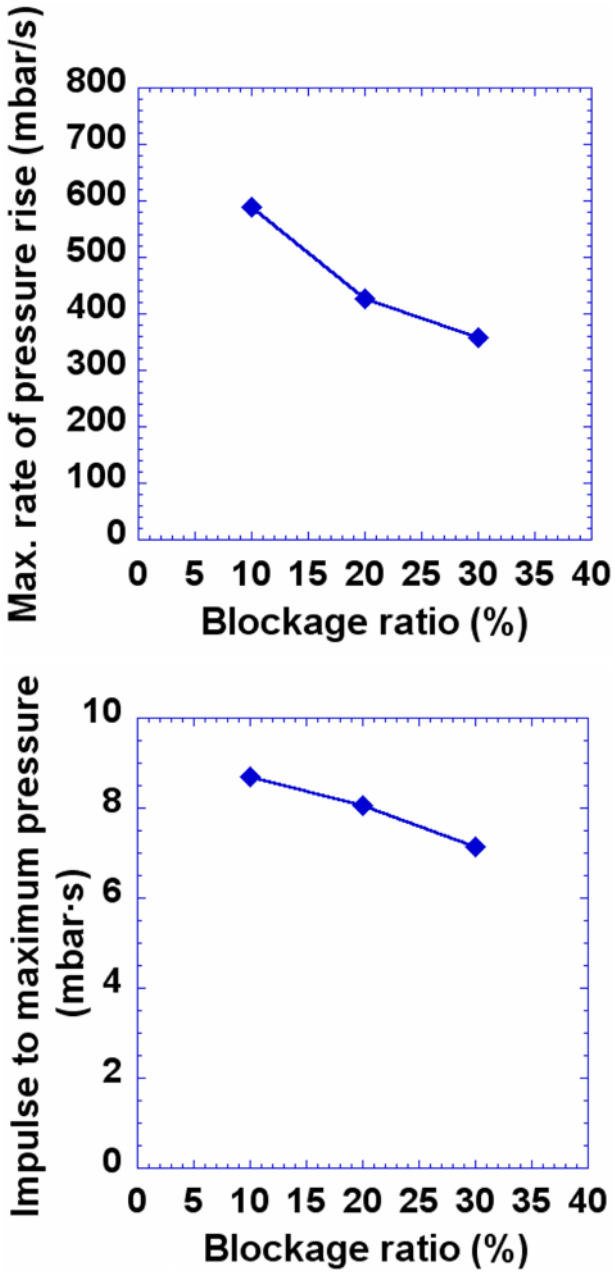

Fig. 5. The maximum rates of pressure rise and impulses to the maximum pressure against different obstruction ratios.

follow the same trend as the results of Park et al. [13]. However, the trend is different compared to those published in the literature for large L/D. This reason may be associated with the characteristics of the chamber, such as the small distance between the ignition point and the chamber exit, and a large transverse vent. In measurements published in the literature for large L/D, the obstacles interact with the flow field, increasing the pressure. However, the propagating flame within the chamber used in study was not fully developed due to the distance from ignition point to the chamber exit being too short. The transverse vent and small distance cause a larger effective vent area in the initial propagation of the flame and hence lower turbulence and lower pressure.

Fig. 5 shows the results of the maximum rate of pressure rise and impulse to peak overpressures for the obstacles. The measurement for the maximum rate of pressure rise was performed by measuring the average slope through the pressure oscillations prior to the maximum pressure. The impulse was measured by integrating the pressure curve to maximum pressure. The highest rate of pressure rise occurred with the 10% blockage ratio, while the lowest occurred with the 30% obstruction. Similarly, the largest impulse occurred with the 10% blockage ratio, while the smallest was obtained with the 30% blockage ratio. The rate of pressure rise and impulse were shown to be a similar trend to the explosion pressure.

2. Influence of Ignition Positions

Fig. 6 shows a sequence of selected high-speed images of flame propagation by four different ignition source positions within the chamber. The ignition source was positioned at the bottom-center of the chamber (bottom ignition, BI), the bottom-corner of the chamber (corner ignition, CI), the side wall of the chamber (side ignition, SI) and near the vent opening (top ignition, TI). Fig. 7 shows the variations of pressure-time histories obtained from the different ignition positions mentioned above.

The flame in the early stages of flame development is an expanding hemisphere from the ignition point for the bottom ignition (BI). At about 80 ms, the leading flame front approached the chamber exit. As the time goes up, the flame propagates laterally along the chamber exit with an increase in flame surface area within the chamber. As the propagating flame fronts reached the chamber side walls, the peak overpressure of 136 mbar occurred at about 304 ms. As the ignition occurred at the bottom-corner of the chamber (CI), the flame was vented at about 70 ms, and the peak overpressure was 82 mbar at about 243 ms. For the side ignition (SI), the venting of burnt products occurred at t=60 ms, and the peak overpressure was 47 mbar at about 266 ms. The venting of burnt gases in the top ignition (TI) positioned close to the vent occurred at almost the same time as the ignition. The flame propagated towards the bottom wall of the chamber from the ignition point, and the peak overpressure was 36 mbar at about 112 ms.

The explosion developments obtained from the four different ignition positions were significantly different. The bottom ignition caused the highest overpressure, while the top ignition the closest to the vent opening caused the lowest overpressure. Also, the time taken to reach the maximum pressure was found to be the shortest with the top ignition, while the longest time was found with the bottom ignition. It is explained that the top ignition provides a greater relief path for burned than for unburned gas venting and hence a rapid pressure decrease in the chamber, and the bottom ignition provides lower heat losses and a higher flame area due to the relatively later contact of the flame with the chamber wall.

CONCLUSIONS

Experimental studies were carried out to investigate the influences of different ignition sources positions and solid wall obstacles within the chamber with a small L/D ratio and large rectangular vent. Four different ignition positions representing bottom ignition, side ignition, corner ignition and top ignition, respectively, and three wall obstacles with blockage ratios ranging from about 10 to 30% were used. The main results obtained from the present work can be summarized as follows:

1. The flame in the early stages of flame propagation for differ-

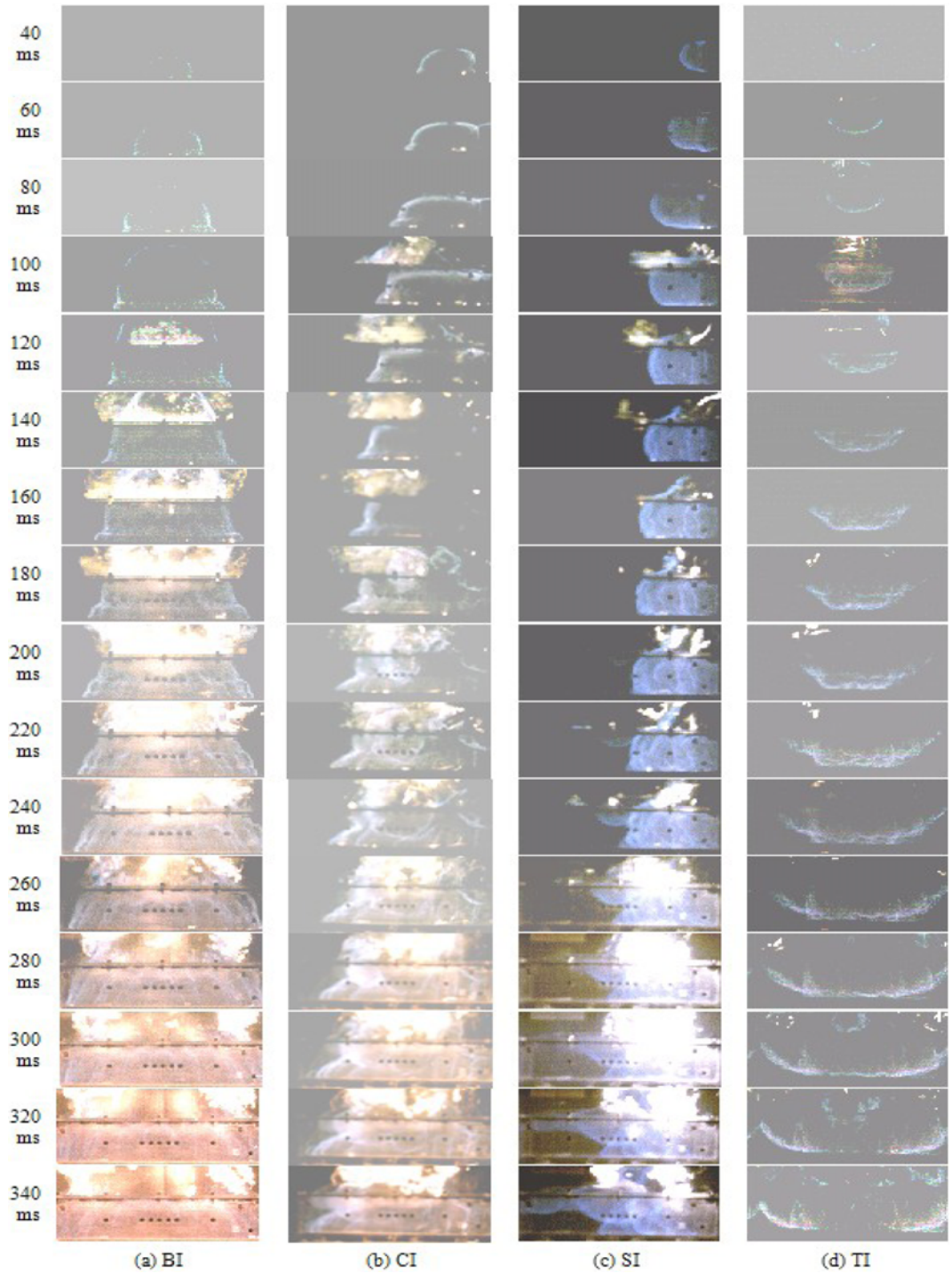

Fig. 6. A sequence of selected high speed images of flame propagation for four different ignition positions: the bottom ignition (BI), corner ignition (CI), side ignition (SI) and top ignition (TI).

ent blockage ratios used is an expanding hemisphere from the ignition point. The delay time of the flame exiting the chamber was shorter with the smallest obstacle, while the longest times occurred with the largest one. The longest flame height and width within the chamber were obtained with the largest obstacle: however, the shortest flame height and width occurred with the smallest obstacle.

2. The obstacle with 10% blockage ratio caused the highest overpressure, while the obstacle with 30% blockage ratio resulted in the lowest overpressure. It was found that the rate of pressure rise and impulse were shown to be a similar trend to the explosion pressure. The different trends of peak pressure at the chamber with low L/D compared to those published in the literature for large L/D may be related to the characteristics of the chamber like the small distance from ignition to the vent in the direction of a propagating flame and the large rectangular vent.

3. The explosion developments obtained from the four different

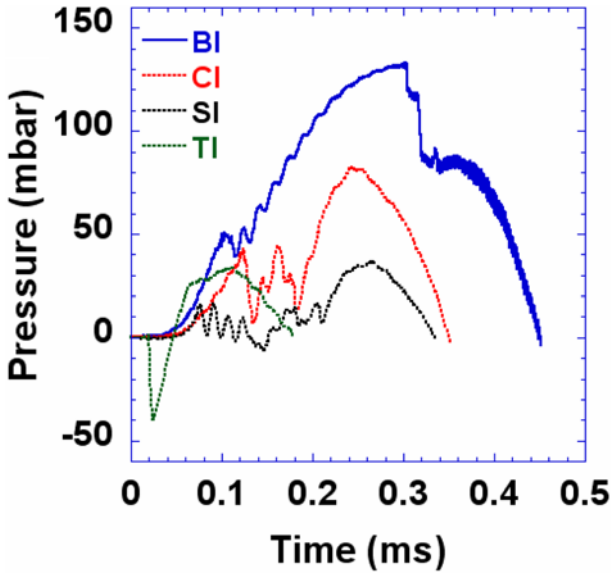

Fig. 7. Comparison of pressure-time history for the different ignition positions.

ignition positions were largely different. The highest overpressure was obtained with the bottom ignition, while the lowest overpressure occurred at the top ignition the closest to the vent opening. Also, the time taken to reach the maximum pressure was found to be the shortest with the top ignition, while the longest time was found with the bottom ignition.

ACKNOWLEDGEMENT

The authors gratefully acknowledge the financial support by R&D Training Centre, Korea Gas Corporation.

REFERENCES

1. D. J. Park and Y. S. Lee, *Korean J. Chem. Eng.*, **26**, 313 (2009).
2. D. K. Pritchard, D. J. Freeman and P. W. Guilbert, *J. Loss Prevention in the Process Industries*, **9**, 205 (1996).
3. H. Phylaktou and G. E. Andrews, *Combust. Sci. Technol.*, **77**, 27 (1991).
4. G. K. Hargrave, S. J. Jarvis and T. C. Williams, *Measurement Sci. Technol.*, **13**, 1036 (2002).
5. I. O. Moen, M. Donato, R. Knystautas and J. H. Lee, *Combust. Flame*, **39**, 21 (1980).
6. A. R. Masri, S. S. Ibrahim, N. Nehzat and A. R. Green, *Exp. Therm. Fluid Sci.*, **21**, 109 (2000).
7. S. S. Ibrahim, G. K. Hargrave and T. C. Williams, *Exp. Therm. Fluid Sci.*, **24**, 99
8. O. C. Ellis and R. V. Wheeler, *J. Chem. Soc.*, **2**, 3215 (1928).
9. W. A. Kirkyby and R. V. Wheeler, *J. Chem. Soc.*, **2**, 3203 (1928).
10. D. M. Solberg, J. A. Pappas and E. Skramstad, *Eighteenth Symposium (International) on Combustion*, Combustion Institute, 1607 (1981).
11. A. R. Green and N. Nehzat, *Proceedings Queensland Mining Industry Heath and Safety Conference*, 240 (1999).
12. J. Kindracki, A. Kobiera, G. Rarata and P. Wolanski, *J. Loss Prevention in the Process Industries*, **20**, 551 (2007).
13. D. J. Park, A. R. Green, Y. S. Lee and Y. C. Chen, *Combust. Flame*, **150**, 27 (2007).
14. D. J. Park, T. S. Lee and Y. S. Lee, *J. KOSOS*, **23**, 81 (2008).